Nonequilibrium Quantum Phase Transition in a Hybrid Atom-Optomechanical System

Niklas Mann[1], M. Reza Bakhtiari[1], Axel Pelster[2], and Michael Thorwart[1]
[1] *I. Institut für Theoretische Physik, Universität Hamburg, Jungiusstraße 9, 20355 Hamburg, Germany*
[2] *Physics Department and Research Center OPTIMAS, Technical University of Kaiserslautern, Erwin-Schrödinger Straße 46, 67663 Kaiserslautern, Germany*
(Dated: 11:30, Thursday 2nd November, 2017)

We consider a hybrid quantum many-body system formed by both a vibrational mode of a nanomembrane, which interacts optomechanically with light in a cavity, and an ultracold atom gas in the optical lattice of the out-coupled light. After integrating over the light field, an effective Hamiltonian reveals a competition between the localizing potential force and the membrane displacement force. For increasing atom-membrane interaction we find a nonequilibrium quantum phase transition from a localized non-motional phase of the atom cloud to a phase of collective motion. Near the quantum critical point, the energy of the lowest collective excitation vanishes, while the order parameter of the condensate becomes non-zero in the symmetry-broken state. The effect occurs when the atoms and the membrane are non-resonantly coupled.

Hybrid quantum systems combine complementary fields of physics, such as solid-state physics, quantum optics and atom physics, in one set-up. Recently, a hybrid atom-optomechanical system [1] has been realized experimentally [2] in which a single mechanical mode of a nanomembrane in an optical cavity is optically coupled to a far distant cloud of cold ^{87}Rb atoms residing in the optical potential of the out-coupled standing wave of the cavity light. As the membrane is displaced, it influences the cavity light by the radiation pressure force, and in the bad-cavity limit, the field follows the membrane displacement adiabatically. This modulates the light phase which leads to a shaking of the atom gas in the lattice. The nanomechanical motion of the membrane then couples non-resonantly to the collective motion of the atoms. The aim of combining ultracold atoms and optomechanics [1, 3–7] is twofold. On the one hand, the ultracold gas can be used for cooling the nanomechanical vibration. On the other hand, emergent phenomena of the correlated quantum many-body system are of interest [8–17].

State-of-the-art optomechanics [3–6] is nowadays able to realize optical feedback cooling [18, 19] of the mechanical oscillator to its quantum-mechanical ground state [20, 21]. Yet, the resolved sideband limit allows ground-state cooling only if the oscillator frequency exceeds the photon loss rate in the cavity [22–24]. Hence, cooling a macroscopic *low-frequency* nanomembrane close to its ground state is so far not possible. One promising concept to overcome this limitation [1, 7] is to utilize an ultracold atom gas to lower the membrane temperature, which has been demonstrated recently [2] by sympathetic cooling down to 650 mK. Current investigations aim to a coherent state transfer of robust quantum entanglement [15].

Apart from cooling the nanomembrane, a particularly interesting fundamental feature is the collective quantum-many body behavior of the hybrid system. For instance, the atom-atom interaction can in principle be coherently modulated by the back-action of the cavity light on the nanooscillator. By this, a long-range interaction emerges which resembles that of a dipolar Bose-Einstein condensate (BEC) [25]. In fact, a simpler hybrid quantum many-body system has also been implemented in the form of a BEC in an optical lattice inside a transversely pumped optical cavity. This configuration shows a Dicke quantum phase transition between a normal phase and a self-organized superradiant phase [26–30]. Moreover, optical bistability [31, 32], a roton-type softening in the atomic dispersion relation [26, 33–35] and optomechanical Bloch oscillations [36] were uncovered.

In this work, motivated by recent experiments [2, 10], we study a hybrid atom-optomechanical setup in the form of a "membrane-in-the-middle" cavity [1, 2, 8–11], see Fig. 1. Importantly, the light-mediated coupling between the atoms and the membrane is non-resonant here. We take the full lattice potential into account and include also atom-atom interaction in the gas, for which we employ a mean-field treatment. The numerical solution of the generalized Gross-Pitaevskii equation confirms the validity of an analytic approach based on a Gaussian condensate profile. Tuning the atom-membrane coupling by changing the laser intensity, a nonequilibrium quantum phase transition (NQPT) occurs between a phase of non-motional atom-membrane states and states of a collective quantum many-body motion. This phase transition is fueled by the competition of the lattice, trying to localize the atoms at the minima, and the mechanical motion of the membrane which tries to shake the atoms. In the vicinity of the quantum critical point, the energy of the lowest collective excitation mode vanishes and the order parameter of the symmetry-broken state becomes non-zero. This mode-softening is accompanied by a roton-type bifurcation of the decay rate of the collective eigenmodes. Indeed, an instability and collective self-oscillations of a coupled atom-membrane device have been reported recently [10].

Model. We consider a single mechanical mode of a nanomembrane with frequency Ω_{m} placed in a low-finesse optical cavity. The outcoupled light of the cavity forms

an optical lattice in which a BEC is placed. In a quasistatic picture, a finite displacement of the membrane changes the position of the lattice sites, leading to a linear displacement force on the atoms which induces transitions to higher motional bands. A back-action of the atomic motion on the membrane is induced by a displacement of their center-of-mass position, which, again, redistributes the photons in the propagating beams. Consequently, the light field intensity inside the cavity changes, which alters the radiation pressure on the membrane. To achieve a sizable atom-membrane coupling, the typical energy scale of the BEC has to match the membrane frequency. This can be controlled by the light intensity which determines the lattice depth. The corresponding set-up is sketched in Fig. 1 and modeled by a standard Hamiltonian, which describes the atom-membrane coupling directly [1, 38]. Adiabatically eliminating the light field in a Born-Markov approximation yields the following effective Hamiltonian

$$H = \int dz \Psi^\dagger(z)\Big[-\omega_R\partial_z^2 + V\sin^2(z) + \frac{g}{2}\Psi^\dagger(z)\Psi(z)\Big]\Psi(z) + \Omega_{\rm m} a^\dagger a - \lambda(a^\dagger + a)\int dz \Psi^\dagger(z)\sin(2z)\Psi(z)\,. \quad (1)$$

Here, $\omega_R = \omega_{\rm L}^2/2m$ is the recoil frequency of an atom with mass m, V is the optical lattice depth, and $\omega_{\rm L}$ the laser frequency. The last term describes the effective atom-membrane coupling with strength λ, where the full structure of the potential is included. $a(a^\dagger)$ and $\Psi(\Psi^\dagger)$ are the bosonic annihilation (creation) operators of the membrane and bosons, which follow the usual algebra, $[a, a^\dagger] = 1$ and $[\Psi(z), \Psi^\dagger(y)] = \delta(z-y)$. Moreover, we have introduced a local atom-atom interaction with strength g. In Eq. (1), we have neglected a term describing a long-range interaction of the form $\sim \sin(z)\sin(z')\sin(z+z')$, which is generated by the photon field. This is justified when the laser frequency is far detuned from the closest atomic transition.

In the condensate regime, a large fraction of the atoms occupies the ground state. Here, we consider weakly interacting atoms that are also weakly coupled to the membrane. Thus, when $g, \lambda \ll \omega_R, \Omega_{\rm m}$, the field operator $\Psi(z)$ can be approximated by a complex function $\psi(z)$ according to $\Psi(z) \simeq \sqrt{N}\psi(z)$, where N denotes the number of atoms. To describe the dynamics of the hybrid system, we use the mean-field Lagrangian density associated to the Hamiltonian and given in Eq. (S9) [38] with the complex number $\langle a\rangle/\sqrt{N} = \alpha = \alpha' + i\alpha''$ and the volume $\mathcal{V}$. We restrict the problem to a single lattice site, i.e., $\int dz \to \int_{-\pi/2}^{\pi/2} dz$ and $\mathcal{V} = \pi$, and use periodic boundary conditions. We proceed in two directions: First, we describe the dynamics analytically with a Gaussian ansatz for the condensate wave function and, second, we numerically solve the ensuing generalized Gross-Pitaevskii equation (GPE) without further approximation. The Euler-Lagrange equations yield

$$i\partial_t\psi = [V\sin^2(z) - \omega_R\partial_z^2 + gN|\psi|^2 - 2\sqrt{N}\lambda\alpha'\sin(2z)]\psi,$$
$$i\partial_t\alpha = (\Omega_{\rm m} - i\gamma)\alpha - \sqrt{N}\lambda\int dz\sin(2z)|\psi|^2\,, \quad (2)$$

where we have introduced a phenomenological damping of the mechanical mode with a rate γ. This is due to finite losses caused by both the clamping of the membrane as well as the radiation pressure and represents the dominant damping channel of the hybrid system.

From the Hamiltonian in Eq. (1), we see that the two potential contributions $V\sin^2(z)$ and $\sqrt{N}\lambda(\alpha + \alpha^*)\sin(2z)$ can compete with each other in a dynamical manner which depends on the back-action of the membrane on the atoms and, thus, on the collective behavior of the atoms. This competition yields to the formation of two different stable phases and a NQPT. It manifests itself in a change of the center-of-mass position of the condensate, or the membrane displacement, equivalently. It is similar to the NQPT in the Dicke-Hubbard model [29, 30], where a self-organized checkerboard lattice occupation is formed above a critical pump strength [26, 27].

To describe a realistic physical set-up (with a motional state coupling), we consider a membrane with $\Omega_{\rm m} = 100\,\omega_R$, which corresponds to a frequency of several hundred kHz. To match the atomic energy scale with $\Omega_{\rm m}$, one has to load the atoms in a deep optical lattice with $V \sim 10^2 - 10^3\omega_R$. In this regime and for weak atomic interaction $Ng \ll \omega_R$, the condensate wave function is well described by a Gaussian profile [37]

$$\psi(z,t) = \left[\frac{1}{\pi\sigma(t)^2}\right]^{1/4} e^{-\frac{[z-\zeta(t)]^2}{2\sigma(t)^2} + i\kappa(t)z + i\beta(t)z^2}\,, \quad (3)$$

with a time-dependent width $\sigma(t)$, centered at the position $\zeta(t)$, as well as with the corresponding phases $\beta(t)$ and $\kappa(t)$. To find the equations of motion of these variational parameters, we determine the lowest cumulants of the condensate probability distribution whose dynamics is described by the generalized GPE (2). To this end, we multiply Eq. (2) (i) by $\psi^*(z,t)(z-\zeta)$ and integrate over z, and, likewise, (ii) by $\psi^*(z,t)\left[(z-\zeta)^2 - \frac{\sigma^2}{2}\right]$ and integrate over z. This yields four linearly independent equations for the variational parameters, two of which are $\dot\zeta = 2\omega_R(\kappa + 2\beta\zeta)$ and $\dot\sigma = 4\omega_R\beta\sigma$. With these, we find

$$\begin{aligned} 2\Omega_{\rm m}^{-1}[\ddot\alpha' + 2\gamma\dot\alpha'] &= -\partial_{\alpha'}E\,,\\ (2\omega_R)^{-1}\ddot\zeta &= -\partial_\zeta E\,,\\ (4\omega_R)^{-1}\ddot\sigma &= -\partial_\sigma E\,, \end{aligned} \quad (4)$$

where the potential energy $E = -\int dz\mathcal{L}|_{\dot\alpha=\dot\psi=0}$ reads

$$E = \frac{gN}{\sqrt{8\pi}\sigma} - \frac{V}{2}\sqrt{e^{-2\sigma^2} - \mathcal{S}^2} - 2\sqrt{N}\lambda\alpha'\mathcal{S} + \frac{\omega_R}{2\sigma^2} + \tilde\Omega_{\rm m}\alpha'^2 \quad (5)$$

with the effective frequency $\tilde{\Omega}_\mathrm{m} = \Omega_\mathrm{m} + \gamma^2/\Omega_\mathrm{m}$. Importantly, we have defined the order parameter $\mathcal{S} = \int dz \sin(2z)|\psi(z)|^2 = e^{-\sigma^2}\sin(2\zeta)$ of the NQPT, which describes the center-of-mass position of the condensate.

Quantum Phase Transition in the Mean-Field Regime. Due to the mechanical damping, the combined system will eventually equilibrate. The steady state is characterized by those values $\alpha_0', \sigma_0, \mathcal{S}_0$ which minimize the potential energy functional $E(\alpha', \sigma, \mathcal{S})$. Indeed, by setting all time-derivatives in Eq. (4) to zero and taking into account Eq. (5), we find the relation $\sqrt{N}\lambda\mathcal{S}_0 = \tilde{\Omega}_\mathrm{m}\alpha_0'$, so that the equilibrium width σ_0 and order parameter $\mathcal{S}_0$ solve the coupled equations $(e^{-2\sigma_0^2} - \mathcal{S}_0^2)^{1/2}[\omega_R + gN\sigma_0/\sqrt{8\pi}] = V\sigma_0^4 e^{-2\sigma_0^2}$ and $\mathcal{S}_0[N\lambda^2(e^{-2\sigma_0^2} - \mathcal{S}_0^2)^{1/2} - N\lambda_{\mathrm{c},V}^2] = 0$ with $N\lambda_{\mathrm{c},V}^2 = \tilde{\Omega}_\mathrm{m}V/4$.

At first, we aim at a qualitative understanding of the system for increasing coupling strength λ. To this end, we use these relations and define the potential energy surface as a function of a single variable, i.e., either σ or $\mathcal{S}$ (or α'). For instance, $E(\sigma) \equiv E(\alpha_0'(\sigma), \sigma, \mathcal{S}_0(\sigma))$ exhibits only a single minimum for $\sigma > 0$. Interestingly enough, however, as a function of the control parameter λ, the energy $E(\mathcal{S})$ has either one stable state or two minima. This is visualized by the normalized potential energy surface $\epsilon(\mathcal{S}, \lambda) = \frac{E(\mathcal{S}) - E(\mathcal{S}_0)}{\max\{E(\mathcal{S}) - E(\mathcal{S}_0)\}}$ in Fig. 2(a). The red curve marks the configuration of minimal energy $\epsilon(\mathcal{S}_0, \lambda) = 0$. There exists a critical coupling λ_c, such that for smaller values $\lambda < \lambda_\mathrm{c}$, the energy surface $E(\mathcal{S})$ forms a single potential well, whereas for $\lambda > \lambda_\mathrm{c}$ we find that $E(\mathcal{S})$ becomes a double well potential with a maximum at $\mathcal{S} = 0$ and two minima.

The resulting order parameter as a function of the atom-membrane coupling λ is shown in Fig. 2(b) for different values of the lattice depth. Here, the solid curves show the results of the analytical approach, whereas the dashed lines refer to the numerical solution of the full GPE. For small values λ, the condensate is symmetrically located around the lattice minima $\zeta_0 = j\pi$ with $j \in \mathbb{Z}$, so the order parameter vanishes, i.e. $\mathcal{S}_0 = 0$. Consequently, the membrane displacement $\alpha_0' \sim \mathcal{S}_0$ vanishes. The NQPT then occurs at a critical coupling λ_c, which follows from solving the implicit equation

$$\omega_R + \frac{gN}{\sqrt{8\pi}}\sqrt{2\,\ln\frac{\lambda_\mathrm{c}}{\lambda_{\mathrm{c},V}}} = 4V\left(\frac{\lambda_{\mathrm{c},V}}{\lambda_\mathrm{c}}\ln\frac{\lambda_\mathrm{c}}{\lambda_{\mathrm{c},V}}\right)^2. \quad (6)$$

Above that critical coupling the atoms start to move away from the positions $j\pi$ to displaced lattice minima defined by $\zeta_0 = j\pi + \tan^{-1}(4\lambda\alpha_0' e^{\sigma_0^2}/V)/2$. The order parameter becomes finite: $\mathcal{S}_0 = \pm\Theta(\lambda - \lambda_\mathrm{c})\sqrt{e^{-2\sigma_0^2} - (\lambda_{\mathrm{c},V}/\lambda)^4}$. In addition, we show the condensate width $\sigma_0(\lambda)$ in Fig. 2(c), which turns out to be independent of λ below λ_c, whereas it decreases in good approximation with $\sim 1/\sqrt{\lambda}$ above λ_c. In accordance with an expansion of the energy surface with respect to the order parameter, all these observables show that the hybrid system undergoes a second order NQPT.

Collective Excitation Modes. Solving the complete set of equations of motion (4) is challenging. Therefore, we linearize these equations, which gives already an insight into the collective excitation energies. To this end we consider small deviations from the stationary state $(\alpha_0', \sigma_0, \mathcal{S}_0(\text{or } \zeta_0))$ in the form of $\alpha'(t) = \alpha_0' + \delta\alpha'(t)$, $\sigma(t) = \sigma_0 + \delta\sigma(t)$ and $\zeta(t) = \zeta_0 + \delta\zeta(t)$. Next, we linearize the equations of motion with respect to the deviations and find the Eqs. (S10) in the Supplementary Material [38]. Interestingly, the oscillation frequencies also indicate the NQPT. Below λ_c, the bare frequency $\omega_\zeta = \sqrt{4\omega_R V}e^{-\sigma_0^2/2}$ of the ζ-mode is independent of λ, whereas, above λ_c, it grows linearly in λ according to $\omega_\zeta = \sqrt{4\omega_R V}e^{-\sigma_0^2}\lambda/\lambda_\mathrm{c}$.

In addition, we determine the eigenmodes of the coupled linear equations of motion (S10) [38] by writing the differential equations in the form of a vector-matrix-multiplication $\dot{\boldsymbol{v}} = \boldsymbol{M}\boldsymbol{v}$. The eigenvalues $\nu_k = i\omega_k - \gamma_k$ of $\boldsymbol{M}$ define the eigenfrequencies ω_k and the decay rates γ_k. Likewise, we estimate the eigenmodes via the GPE by considering small deviations from the ground state according to $\psi(z,t) = e^{i\mu t}[\psi_0(z) + \delta\psi(z,t)]$ and $\alpha(t) = \alpha_0 + \delta\alpha(t)$. Linearization with respect to the deviations results in a differential equation of the form $\dot{\boldsymbol{u}}(z) = \boldsymbol{M}_\mathrm{GP}\boldsymbol{u}(z)$, where the eigenvalues of $\boldsymbol{M}_\mathrm{GP}$ provide the eigenfrequencies and the decay rates [38].

The eigenfrequencies of the collective excitations without interatomic collisions are shown in Fig. 3(a) and the corresponding decay rates in Fig. 3(c) as a function of the atom-membrane coupling strength. A zoom around λ_c is shown in Fig. 3(b) and (d). The dashed lines show the frequency (rate) calculated in the GPE approach, whereas the solid lines refer to the analytical results. Approaching the critical coupling, the lowest excitation frequency (red, triangles) in Fig. 3(a) and (b) decreases with a roton-type behavior according to $\sim\sqrt{1-\lambda^2/\lambda_\mathrm{c}^2}$. At the same time, the corresponding decay rate increases up to a maximum at λ_c. In a narrow range $\Delta\lambda \simeq 0.1\,\omega_R$ around λ_c, a bifurcation of the decay rate can be observed, whereas the lowest excitation frequency is constantly zero. Such a behavior is well known from atomic ensembles with long-range interactions [34, 35, 39, 40] which, in the present case, are mediated by the membrane. Indeed, adiabatically eliminating the membrane mode introduces a long-range interaction potential that takes the form $G(z,z') = G_0\sin(2z)\sin(2z')$ with $G_0 = -2\lambda^2/\tilde{\Omega}_\mathrm{m}$. Finally, we note that although all figures refer to the case $g = 0$, we find no qualitative difference when (weakly) interacting atoms are considered. In fact, even for $Ng \lesssim 0.1V$, the results agree quantitatively.

Experimental realization. An experimental observation of this NQPT is possible on the basis of existing experimental set-ups, e.g., in Ref. [11]. The effective atom-membrane coupling does not have to be resonant and can

be tuned by modifying the intensity of the laser which determines the lattice depth V. Moreover, an independent tuning of λ can be achieved by applying a second laser which is slightly misaligned relative to the first one and which generates an optical lattice of the same periodicity but shifted by $\pi/2$. The commonly accessible observable is the momentum distribution

$$n(k) = N \int dz e^{ik(z-\zeta_0)} |\psi(z)|^2 = N e^{-(k\sigma_0/2)^2} \qquad (7)$$

of the atoms shown in Fig. 4(a), together with its width for varying λ in Fig. 4(c). Below λ_c, the width is constant, while it increases monotonically for $\lambda > \lambda_c$. In addition, the NQPT can also be detected by measuring the eigenfrequency ω_3 of the membrane shown in Fig. 4(b). It is accessible spectroscopically and can be measured with a high relative precision of much below 1%, so that the cusp at λ_c should be clearly resolvable.

Conclusions. We have shown that a hybrid atom-optomechanical system possesses a nonequilibrium quantum phase transition between phases of different collective behavior. Based on a Gross-Pitaevskii like mean-field approach, the steady-state characteristics of an ultracold atomic condensate in an optical lattice, whose motion is non-resonantly coupled to a single mechanical vibrational mode of a spatially distant membrane, has been analyzed. The coupling between both parts occurs via the light field of a common laser. Below the critical effective atom-membrane coupling λ_c, the atoms in the combined atom-membrane ground state are symmetrically distributed around their lattice minima. Tuning the atom-membrane coupling above the critical value induces a nonequilibrium quantum phase transition to a symmetry-broken state in which the atomic center-of-mass and membrane displacements are all either positive or negative. In the vicinity of the NQPT, the lowest excitation mode shows roton-type characteristics in the excitation frequency, a mode softening and a bifurcation of the decay rate.

Acknowledgments. This work was supported by the Deutsche Forschungsgemeinschaft (N.M.), by the DFG Collaborative Research Center 928 "Light-induced dynamics and control of correlated quantum systems" (M.R.B.) and the DFG Collaborative Research Center/TransRegio 185 "Open System Control of Atomic and Photonic Matter" (A.P.). We thank Christoph Becker, Alexander Schwarz and Hai Zhong for useful discussions on experimental set-ups.

[1] B. Vogell, K. Stannigel, P. Zoller, K. Hammerer, M. T. Rakher, M. Korppi, A. Jöckel, and P. Treutlein, Phys. Rev. A **87**, 023816 (2013).
[2] A. Jöckel, A. Faber, T. Kampschulte, M. Korppi. M. T. Rakher, and P. Treutlein, Nature Nano. **10**, 55 (2015).
[3] M. Aspelmeyer, T. J. Kippenberg, and F. Marquardt, Rev. Mod. Phys. **86**, 1391 (2014).
[4] T. J. Kippenberg and K. J. Vahala, Science **321**, 1172 (2008).
[5] I. Favero and K. Karrai, Nat. Photonics **3**, 201 (2009).
[6] M. Aspelmeyer, S. Gröblacher, K. Hammerer, and N. Kiesel, J. Opt. Soc. Am. B **27**, A189 (2010).
[7] B. Vogell, T. Kampschulte, M. T. Rakher, A. Faber, P. Treutlein, K. Hammerer, and P. Zoller, New J. Phys. **17**, 043044 (2015).
[8] M. Wallquist, K. Hammerer, P. Rabl, M. Lukin, and P. Zoller, Phys. Scr. **T137**, 014001 (2009).
[9] D. Hunger, S. Camerer, M. Korppi, A. Jöckel, T. Hänsch, and P. Treutlein, C. R. Phys. **12**, 871 (2011).
[10] A. Vochezer, T. Kampschulte, K. Hammerer, and P. Treutlein, `arxiv:1705.10098` (2017).
[11] H. Zhong, G. Fläschner, A. Schwarz, R. Wiesendanger, P. Christoph, T. Wagner, A. Bick, C. Staarmann, B. Abeln, K. Sengstock, and C. Becker, Rev. Sci. Instrum. **88**, 023115 (2017).
[12] D. Meiser and P. Meystre, Phys. Rev. A **73**, 033417 (2006).
[13] C. Genes, D. Vitali, and P. Tombesi, Phys. Rev. A **77**, 050307 (2008).
[14] H. Ian, Z. R. Gong, Yu-xi Liu, C. P. Sun, and F. Nori, Phys. Rev. A **78**, 013824 (2008).
[15] K. Hammerer, M. Aspelmeyer, E. S. Polzik, and P. Zoller, Phys. Rev. Lett. **102**, 020501 (2009).
[16] K. Hammerer, M. Wallquist, C. Genes, M. Ludwig, F. Marquardt, P. Treutlein, P. Zoller, J. Ye, and H. J. Kimble, Phys. Rev. Lett. **103**, 063005 (2009).
[17] M. Paternostro, G. De Chiara, and G. M. Palma, Phys. Rev. Lett. **104**, 243602 (2010).
[18] P.-F. Cohadon, A. Heidmann, and M. Pinard, Phys. Rev. Lett. **83**, 3174 (1999).
[19] D. Kleckner and D. Bouwmeester, Nature **444**, 75 (2006).
[20] J. D. Teufel, T. Donner, D. Ji, J. W. Harlow, M. S. Allman, K. Cicak, A. J. Sirois, J. D. Whittaker, K. W. Lehnert, and R. W. Simmonds, Nature **475**, 359 (2011).
[21] J. Chan, T. P. Mayer Alegre, A. H. Safavi-Naeini, J. T. Hill, A. Krause, S. Gröblacher, M. Aspelmeyer, and O. Painter, Nature **478**, 88 (2011).
[22] W. Neuhauser, M. Hohenstatt, P. Toschek, and H. Dehmelt, Phys. Rev. Lett. **41**, 233 (1978).
[23] F. Marquardt, J. P. Chen, A. A. Clerk, and S. M. Girvin, Phys. Rev. Lett. **99**, 093902 (2007).
[24] A. Schliesser, R. Rivière, G. Anetsberger, O. Arcizet, and T. J. Kippenberg, Nature Phys. **4**, 415 (2008).
[25] T. Lahaye, C. Menotti, L. Santos, M. Lewenstein, and T. Pfau, Rep. Prog. Phys. **72**, 126401 (2009).
[26] D. Nagy, G. Szirmai, and P. Domokos, Eur. Phys. J. D **48**, 127 (2008).
[27] C. Maschler, I. B. Mekhov, and H. Ritsch, Eur. Phys. J. D **46**, 545 (2008).
[28] K. Baumann, C. Guerlin, F. Brennecke, and T. Esslinger, Nature **464**, 1301 (2010).
[29] M. Reza Bakhtiari, A. Hemmerich, H. Ritsch, and M. Thorwart, Phys. Rev. Lett. **114**, 123601 (2015).
[30] J. Klinder, H. Keßler, M. Reza Bakhtiari, M. Thorwart, and A. Hemmerich, Phys. Rev. Lett. **115**, 230403 (2015).
[31] S. Gupta, K. L. Moore, K. W. Murch, and D. M. Stamper-Kurn, Phys. Rev. Lett. **99**, 213601 (2007).
[32] S. Ritter, F. Brennecke, K. Baumann, T. Donner, C. Guerlin, and T. Esslinger, Appl. Phys. B **95**, 213 (2009).

[33] B. Öztop, M. Bodyuh, Ö. E. Müsecaplıoğlu, and H. E. Türeci, New J. Phys. **14**, 085011 (2012).
[34] R. Mottl, F. Brennecke, K. Baumann, R. Landig, T. Donner, and T. Esslinger, Science **336**, 1570 (2012).
[35] J. Lénoard, A. Morales, P. Zupancic, T. Donner, and T. Esslinger, `arXiv:1704.05803` (2017).
[36] H. Keßler, J. Klinder, B. Prasanna Venkatesh, C. Georges, and A. Hemmerich, New J. Phys. **18**, 102001 (2016).
[37] H. Al-Jibbouri and A. Pelster, Phys. Rev. A **88**, 033621 (2013).
[38] See Supplemental Material at [URL will be inserted by publisher] for details.
[39] L. Santos, G. V. Shlyapnikov, and M. Lewenstein, Phys. Rev. Lett. **90**, 250403 (2003).
[40] S. Giovanazzi and D. H. J. O'Dell, Eur. Phys. J. D **31**, 439 (2004).

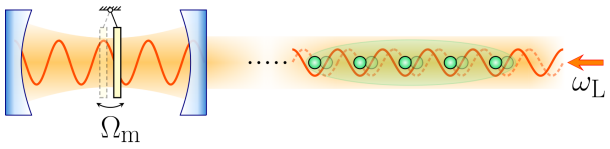

FIG. 1. Sketch of the hybrid system. A nanomechanical membrane in an optical cavity is optically coupled to the vibrational motion of a distant atom gas.

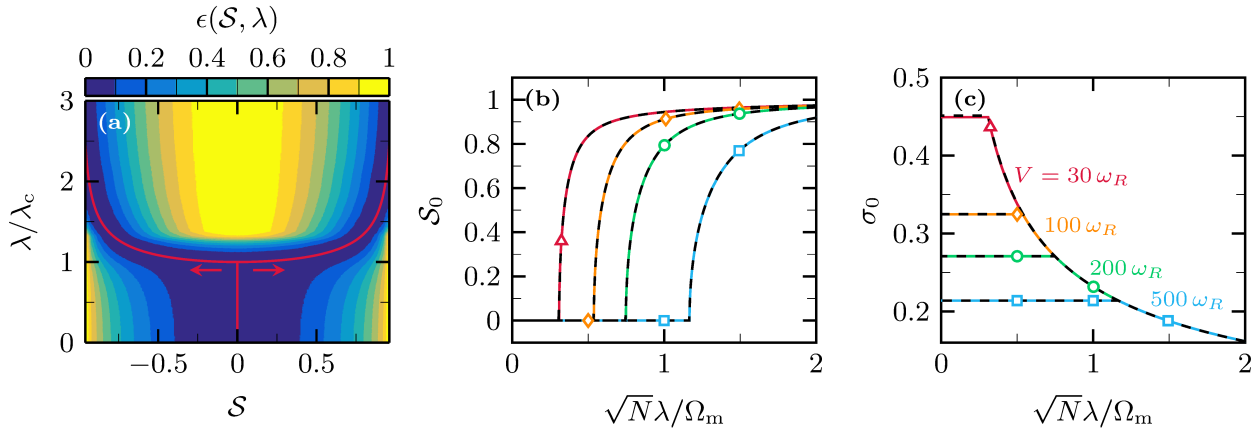

FIG. 2. (a) Normalized potential energy surface $\epsilon(\mathcal{S},\lambda)$ as a function of $\mathcal{S}$ and λ for $V = 200\,\omega_R$. The red line indicates the minimum $\epsilon(\mathcal{S}_0,\lambda) = 0$. (b) Positive value of $\mathcal{S}_0$ and (c) condensate width σ_0 as a function of λ for different values V as indicated in (c). The dashed curves show the GPE results for comparison. For all panels, we have used $g = 0$, $\Omega_{\rm m} = 100\,\omega_R$ and $\gamma = 20\,\omega_R$

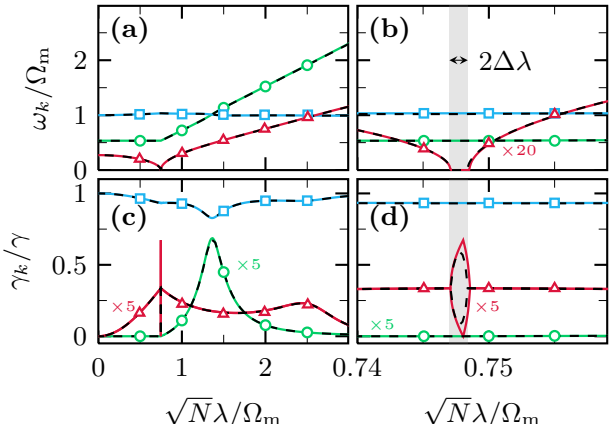

FIG. 3. (a), (b) Frequencies of collective excitations, and, (c), (d) decay rates of the collective eigenmodes (some curves are scaled by the factors indicated). Panels (b) and (d) show a zoom around $\lambda_{\rm c}$ with width $\Delta\lambda \simeq 0.1\,\omega_R$. Different colors correspond to different eigenmodes. The blue curves correspond to the membrane mode, the green curves to the condensate width mode and the red curve to the atomic displacement excitation. The dashed curves show the GPE results. The parameters are $V = 200\,\omega_R$, $\Omega_{\rm m} = 100\,\omega_R$, $\gamma = 20\,\omega_R$ and $g = 0$.

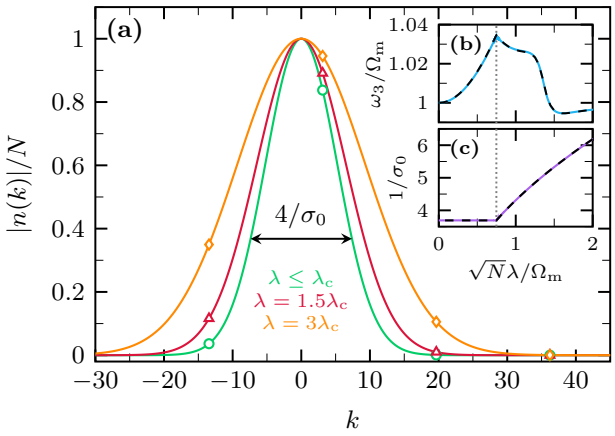

FIG. 4. (a) Momentum distribution $|n(k)|$ of the atoms in a single well below and above the critical coupling λ_c. (b) Zoom to the 'membrane' excitation frequency ω_3 of Fig. 3 (blue squares). (c) Width of $|n(k)|$ in dependence of λ. The dotted vertical line indicates λ_c. The parameters are $V = 200\,\omega_R$, $\Omega_m = 100\,\omega_R$, $\gamma = 20\,\omega_R$ and $g = 0$.

Nonequilibrium Quantum Phase Transition in a Hybrid Atom-Optomechanical System

- Supplemental Material -

Niklas Mann[1], M. Reza Bakhtiari[1], Axel Pelster[2], and Michael Thorwart[1]
[1] *I. Institut für Theoretische Physik, Universität Hamburg, Jungiusstraße 9, 20355 Hamburg, Germany*
[2] *Physics Department and Research Center OPTIMAS, Technical University of Kaiserslautern, Erwin-Schrödinger Straße 46, 67663 Kaiserslautern, Germany*
(Dated: 11:32, Thursday 2nd November, 2017)

I. EFFECTIVE HAMILTONIAN OF THE HYBRID SYSTEM

We start from the Hamiltonian [1]

$$H = H_{\rm m} + H_{\rm a} + H_{\rm l} + H_{\rm m\text{-}l} + H_{\rm a\text{-}l}\,. \tag{S1}$$

The first three terms describe the free time evolution of the single mechanical mode of the nanomembrane, the atomic condensate and the light field, respectively. In addition, the coupling between the light field and the atoms and between the light field and the membrane is denoted by $H_{\rm a\text{-}l}$ and $H_{\rm m\text{-}l}$, respectively. The single membrane mode is modeled as a harmonic oscillator with frequency $\Omega_{\rm m}$ with the Hamiltonian

$$H_{\rm m} = \Omega_{\rm m} a^\dagger a\,, \tag{S2}$$

and the atomic condensate by the usual many-body Hamiltonian in second quantization

$$H_{\rm a} = -\omega_R \int dz\, \Psi^\dagger(z)\partial_z^2\Psi(z) + \frac{g}{2}\int dz\,|\Psi(z)|^4\,, \tag{S3}$$

where $\omega_R = \omega_{\rm L}^2/2m$ is the recoil frequency, $\omega_{\rm L}$ the laser frequency and g the local interaction strength. The light modes are included over a bandwidth 2θ around the laser frequency by the Hamiltonian

$$H_{\rm l} = \int_{\omega_{\rm L}-\theta}^{\omega_{\rm L}+\theta} d\omega\, \Delta_\omega b_\omega^\dagger b_\omega\,, \tag{S4}$$

with $\Delta_\omega = \omega - \omega_L$. The above defined operators fulfill the usual bosonic commutation relations, i.e., $[a, a^\dagger] = 1$, $[b_\omega, b_\nu^\dagger] = \delta_{\omega\nu}$ and $[\Psi(z), \Psi^\dagger(z')] = \delta(z - z')$.

By a linear replacement $b_\omega \to b_\omega + \delta(\omega - \omega_{\rm L})e^{-i\omega_{\rm L}t}\alpha_{\rm L}$ with field strength $\alpha_{\rm L}$, the external laser drive is included. Then, linearizing around $\alpha_{\rm L}$ leads to the membrane-light coupling

$$H_{\rm m\text{-}l} = \lambda_{\rm m}(a + a^\dagger)\int \frac{d\omega}{\sqrt{2\pi}}\,(b_\omega + b_\omega^\dagger)\,, \tag{S5}$$

with the coupling strength $\lambda_{\rm m}$. On the other hand, the laser field induces a Stark shift in the ground state of the atoms. Consequently, the atom-light coupling is described by the interaction Hamiltonian

$$\begin{aligned} H_{\rm a\text{-}l} &= V\int dz\,\Psi^\dagger(z)\sin^2(z)\Psi(z) \\ &+ \lambda_{\rm a}\int\frac{d\omega}{\sqrt{2\pi}}\,(b_\omega + b_\omega^\dagger)\int dz\,\Psi^\dagger(z)\sin(z)\sin(\tfrac{\omega}{\omega_{\rm L}}z)\Psi(z)\,. \end{aligned} \tag{S6}$$

with the optical lattice depth V and the atom-light coupling strength $\lambda_{\rm a}$. To obtain an effective Hamiltonian for the atom-membrane coupling, the idea is the following. First, we derive the Heisenberg equation for the field quadrature $x_\omega = (b_\omega + b_\omega^\dagger)/\sqrt{2}$

$$\begin{aligned} \ddot{x}_\omega + \Delta_\omega^2 x_\omega &= -\frac{\lambda_{\rm m}\Delta_\omega}{\sqrt{\pi}}(a + a^\dagger) \\ &- \frac{\lambda_{\rm a}\Delta_\omega}{\sqrt{\pi}}\int dz\Psi^\dagger(z)\sin(z)\sin(\tfrac{\omega}{\omega_{\rm L}}z)\Psi(z)\,. \end{aligned} \tag{S7}$$

Then, we insert the formal solution of (S7) in the equations of motion for a and $\Psi(z)$. The emerging integrals over the field modes ω are of the form

$$\int d\omega\sin(\tfrac{\Delta_\omega}{\omega_L}\tau)\sin(\tfrac{\omega}{\omega_L}z)\underset{\theta\to\infty}{\longrightarrow}\pi\cos(z)[\delta(\tau - z) - \delta(\tau + z)]\,. \tag{S8}$$

Finally, neglecting the advanced term and using the relation $\cos(z)\sin(z) = \sin(2z)/2$, one may insert the result in the equations of motion for a, Ψ and read off the effective Hamiltonian given in Eq. (1) of the main text with the effective coupling $\lambda = \lambda_{\rm a}\lambda_{\rm m}/2$.

II. LAGRANGIAN DENSITY

The Lagrangian density of the hybrid system can be directly inferred from the effective Hamiltonian in Eq. (1) in the main paper. It reads

$$\mathcal{L} = \frac{1}{\mathcal{V}}\Big[\frac{i}{2}(\dot\alpha\alpha^* - \alpha\dot\alpha^*) - \Omega_{\rm m}\alpha^*\alpha\Big] + \frac{i}{2}(\dot\psi\psi^* - \psi\dot\psi) - \Big[\omega_R|\partial_x\psi|^2 + V\sin^2(x)|\psi|^2 + \frac{gN}{2}|\psi|^4 - \sqrt{\lambda}(\alpha + \alpha^*)\sin(2x)|\psi|^2\Big]\,, \tag{S9}$$

with the complex number $\langle a\rangle/\sqrt{N} = \alpha = \alpha' + i\alpha''$ and the volume $\mathcal{V}$.

III. COLLECTIVE EXCITATIONS AND COLLECTIVE EIGENMODES

To obtain physical insight, we consider the set of equations of motion (4) given in the main text. Their explicit solution is not possible analytically, but we can perform an eigenmode analysis. For this, we linearize the Eqs. (4) by considering small deviations from the stationary state $(\alpha_0', \sigma_0, \mathcal{S}_0(\text{or } \zeta_0))$ in the form of $\alpha'(t) = \alpha_0' + \delta\alpha'(t)$, $\sigma(t) = \sigma_0 + \delta\sigma(t)$ and $\zeta(t) = \zeta_0 + \delta\zeta(t)$. The subsequent linearization with respect to the deviations yields

$$\begin{aligned} \delta\ddot{\alpha}' + 2\gamma\delta\dot{\alpha}' + \tilde{\Omega}_\mathrm{m}\Omega_\mathrm{m}\delta\alpha' &= b_\zeta\delta\zeta - b_\sigma\delta\sigma\,, \\ \delta\ddot{\zeta} + \omega_\zeta^2\delta\zeta &= c_\alpha\delta\alpha'\,, \\ \delta\ddot{\sigma} + \omega_\sigma^2\delta\sigma &= -d_\alpha\delta\alpha'\,, \end{aligned} \tag{S10}$$

with the frequencies $\omega_\zeta^2 = 4\omega_R V e^{-2\sigma_0}/w_0$ and $\omega_\sigma^2 = 4\omega_R[3\omega_R/\sigma_0^4 + Ve^{-2\sigma_0}(1-2\sigma_0^2)/w_0 + gN/\sqrt{2\pi}\sigma_0^3]$ where $w_0^2 = e^{-2\sigma_0^2} - \mathcal{S}_0^2$. Moreover, we have defined the coupling constants $b_\zeta = 2\sqrt{N}\lambda\Omega_\mathrm{m}w_0$, $b_\sigma = 2\sqrt{N}\lambda\Omega_\mathrm{m}\sigma_0\mathcal{S}_0$, $c_\alpha = 8\sqrt{N}\lambda\omega_R w_0$, and $d_\alpha = 16\omega_R\sqrt{N}\lambda\sigma_0\mathcal{S}_0$.

In order to determine the collective excitation spectrum within a harmonic analysis, we define the vector $\boldsymbol{v} = (\delta\alpha', \delta\dot{\alpha}', \delta\zeta, \delta\dot{\zeta}, \delta\sigma, \delta\dot{\sigma})^T$ and rewrite Eq. S10 in the form $\dot{\boldsymbol{v}} = \boldsymbol{M}\boldsymbol{v}$, with the matrix

$$\boldsymbol{M} = \begin{pmatrix} 0 & 1 & 0 & 0 & 0 & 0 \\ -\Omega_\mathrm{m}^2 - \gamma^2 & -2\gamma & b_\zeta & 0 & -b_\sigma & 0 \\ 0 & 0 & 0 & 1 & 0 & 0 \\ c_\alpha & 0 & -\omega_\zeta^2 & 0 & 0 & 0 \\ 0 & 0 & 0 & 0 & 0 & 1 \\ -d_\alpha & 0 & 0 & 0 & -\omega_\sigma^2 & 0 \end{pmatrix}. \tag{S11}$$

Below the critical point, the matrix $\boldsymbol{M}$ becomes block-diagonal as $d_\alpha = b_\sigma = 0$. In the limit of zero damping, this reduces to an analytically solvable eigenvalue problem of the matrix

$$\boldsymbol{M}' = \begin{pmatrix} 0 & 1 & 0 & 0 \\ -\Omega_\mathrm{m}^2 & 0 & b_\zeta & 0 \\ 0 & 0 & 0 & 1 \\ c_\alpha & 0 & -\omega_\zeta^2 & 0 \end{pmatrix}. \tag{S12}$$

$\boldsymbol{M}'$ has the four imaginary eigenvalues ν_i given by the relation $\nu^2 = -\left(\Omega_\mathrm{m}^2 + \omega_\zeta^2 \pm \sqrt{(\Omega_\mathrm{m}^2 - \omega_\zeta^2)^2 + 4b_\zeta c_\alpha}\right)/2$. When $(\Omega_\mathrm{m}^2 - \omega_\zeta^2)^2 \gg b_\zeta c_\alpha$, which is well satisfied for the parameters chosen in this work, the eigenvalues can be estimated to

$$\begin{aligned} \nu_{1,2} &= \pm i\Omega_\mathrm{m}\sqrt{1 + (\lambda/\lambda_\mathrm{c})^2}\,, \\ \nu_{3,4} &= \pm i\omega_\zeta\sqrt{1 - (\lambda/\lambda_\mathrm{c})^2}\,, \end{aligned} \tag{S13}$$

where $b_\zeta c_\alpha/\Omega_\mathrm{m}^2\omega_\zeta^2 = (\lambda/\lambda_\mathrm{c})^2$ has been used. The remaining two eigenvalues of the full matrix $\boldsymbol{M}$ are given by $\nu_{5,6} = \pm i\omega_\sigma$.

IV. COLLECTIVE EXCITATIONS IN THE GROSS-PITAEVKSII EQUATION (GPE)

A harmonic analysis can also be carried out within the GPE. The collective excitation spectrum follows by considering deviations from the stationary state (ψ_0, α_0) in the form $\psi(z,t) = e^{-i\mu t}[\psi_0(z) + \delta\psi(z,t)]$ and $\alpha(t) = \alpha_0 + \delta\alpha(t)$. Without loss of generality, $\psi_0(z)$ can be chosen to be real valued. Then, linearizing the coupled equations (3) of the main text with respect to the deviations, the Bogoliubov-de Gennes equations

$$\begin{aligned} i\partial_t\delta\psi(z) &= [h_0(z) + 2gN\psi_0^2(z)]\delta\psi(z) + gN\psi_0^2(z)\delta\psi^*(z) \\ &\quad - \lambda\sin(2z)\psi_0(z)[\delta\alpha + \delta\alpha^*]\,, \\ i\partial_t\delta\alpha &= [\Omega_\mathrm{m} - i\gamma]\delta\alpha - N\lambda\mathcal{Q}[\delta\psi + \delta\psi^*]\,, \end{aligned} \tag{S14}$$

are obtained, with the linear operator $\mathcal{Q}[f] = \int dz\,\psi_0(z)\sin(2z)f(z)$ and $h_0(z) = -\omega_R\partial_z^2 + V\sin^2(z) + Ng\psi_0^2(z) - \lambda(\alpha_0 + \alpha_0^*)\sin(2z) - \mu$.

The set of coupled differential equations (S14) couples the deviations to their complex conjugates. In that sense, the solutions are of the form $\delta\alpha(t) = \sum_k[e^{-i\nu_k t}\delta\alpha_{+,k} + e^{i\nu_k t}\delta\alpha_{-,k}^*]$ and $\delta\psi(z,t) = \sum_k[e^{-i\nu_k t}u_k(z) + e^{i\nu_k t}v_k^*(z)]$ with complex frequencies ν_k. Within this ansatz, the frequencies are determined by solving the eigenvalue problem

$$\nu_k\boldsymbol{w}_k(z) = \boldsymbol{M}_\mathrm{GP}(z)\boldsymbol{w}_k(z)\,, \tag{S15}$$

with the vector $\boldsymbol{w}_k(z) = (\delta\alpha_{+,k}, u_k(z), \delta\alpha_{-,k}, v_k(z))^T$ and the matrix

$$\boldsymbol{M}_\mathrm{GP}(z) = \begin{pmatrix} X & Y \\ -Y & -X \end{pmatrix} \tag{S16}$$

where

$$\begin{aligned} X &= \begin{pmatrix} \Omega_\mathrm{m} - i\gamma & -N\lambda\mathcal{Q} \\ -\lambda\sin(2z)\psi_0 & h_0 + 2gN\psi_0^2 \end{pmatrix}, \\ Y &= \begin{pmatrix} 0 & -N\lambda\mathcal{Q} \\ -\lambda\sin(2z)\psi_0 & gN\psi_0^2 \end{pmatrix}. \end{aligned} \tag{S17}$$

The eigenvalues of $\boldsymbol{M}_\mathrm{GP}(z)$ appear in pairs, such that if ν_k is an eigenvalue, the negative complex conjugate $-\nu_k^*$ is also an eigenvalue.

V. MOMENTUM DISTRIBUTION OF THE ATOMS

The momentum distribution of the atoms in a single lattice site is given in Eq. (7) of the main text. If we also take into account that we have, in fact, a periodic potential with M lattice sites, the momentum distribution $n_\mathrm{lat}(k)$ of the atoms can be calculated as follows. We start from the atomic density in the lattice

$$n_\mathrm{lat}(z) \simeq \frac{N}{M}\sum_{l=0}^{M-1}\frac{1}{\sqrt{\pi}\sigma_0}e^{-(z-\zeta_0-\pi l)^2/\sigma_0^2}\,, \tag{S18}$$

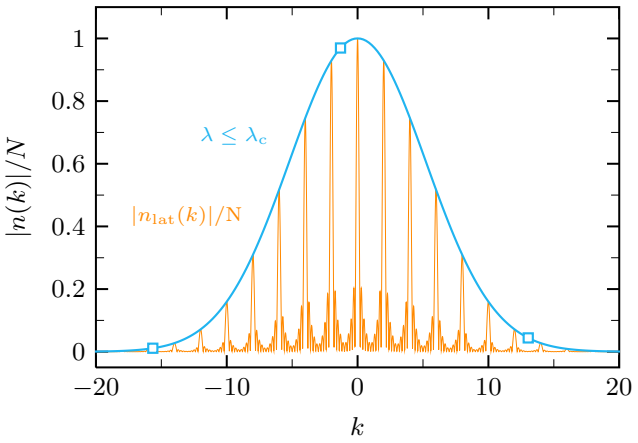

FIG. S1. Momentum distributions of atoms in a single lattice site $|n(k)|$, and of the full lattice $n_{\rm lat}(k)$ for $M = 10$ sites below the critical coupling λ_c. The parameters are $V = 200\,\omega_R$, $\Omega_m = 100\,\omega_R$, $\gamma = 20\,\omega_R$ and $g = 0$.

where M denotes the number of lattice sites (potential wells). The corresponding momentum distribution of the atoms in the lattice is then

$$n_{\rm lat}(k) = \int dz e^{ikz} n_{\rm lat}(z) \equiv f(k) n(k) e^{ik\zeta_0} \tag{S19}$$

with the momentum distribution of a single lattice site

$$n(k) = N \int dz e^{ik(z-\zeta_0)} |\psi(z)|^2 = N e^{-(k\sigma_0/2)^2} \tag{S20}$$

and the form factor

$$|f(k)| = \frac{\sin(\pi M k/2)}{M \sin(\pi k/2)}\,. \tag{S21}$$

The atomic momentum distribution $n_{\rm lat}(k)$ of the whole lattice is shown in Fig. S1 together with the single site momentum distribution $n(k)$.

[1] B.Vogell, K. Stannigel, P. Zoller, K. Hammerer, M. T. Rakher, M. Korppi, A. Jöckel, P. Treutlein, Phys. Rev. A **87**, 023816 (2013).